Hyperbranched Azo-Polymers Synthesized by Azo-Coupling Reaction of an AB_2 Monomer and Postpolymerization Modification

Pengchao Che, Yaning He, and Xiaogong Wang*

Department of Chemical Engineering and School of Materials Science and Engineering, Tsinghua University, Beijing, P. R. China 100084

Received June 1, 2005; Revised Manuscript Received August 15, 2005

ABSTRACT: A series of hyperbranched azo-polymers have been synthesized by two-stage azo-coupling reactions, in which a hyperbranched precursor azo-polymer (HPAP) was prepared by step-growth polymerization of an AB_2 monomer through azo-coupling reaction and then was further modified by postpolymerization azo-coupling reaction at the peripheral groups. The AB_2 monomer, di[2-(*N*-ethylanilino)ethyl]-5-aminoisophthalate, was synthesized from the nucleophilic substitution reaction between *N*-ethyl-*N*-(2-chloroethyl)aniline and 3,5-bis(carboxyl)aniline. On the basis of the monomer, HPAP was prepared by step-growth polycondensation of the diazonium salt of the AB_2 monomer. The hyperbranched precursor polymer was then reacted with diazonium salts of 4-nitroaniline, 4-aminobenzoic acid, and 4-aminobenzonitrile to introduce different types of donor−acceptor azo-chromophores at the peripheral positions. The structure and properties of the azo-polymers were characterized by the spectroscopic methods and thermal analysis. The hyperbranched azo-polymers were used to fabricate surface relief gratings (SRGs) by exposing spin-coated thin films of the polymers to an interference pattern of Ar^+ laser beams at modest intensity (150 mW/cm^2). The type of electron-withdrawing groups in the para-positions of the terminal azobenzene units shows a significant effect on the SRG inscription rate. The synthetic scheme demonstrated in this work is a feasible way to prepare a variety of hyperbranched azo-polymers under extremely mild conditions. The hyperbranched azo-polymers can potentially be used for applications such as reversible optical data storage, photoswitching, sensors, and other photodriven devices.

Introduction

Hyperbranched polymers, as one type of dendritic polymers, have received great attention during the past decade.[1−4] Similar to other dendritic polymers, hyperbranched polymers are characterized by a highly branched backbone and a large number of terminal functional groups. Because of the structural characteristics, hyperbranched polymers show many interesting properties of the dendritic polymers, such as good solubility, low melt and solution viscosity, and the feasibility to be further modified through various chemical reactions of the peripheral groups.[5−9] In comparison with dendrimers, which have a well-controlled size and shape and are prepared by multistep reactions through a divergent or convergent scheme, hyperbranched polymers have less regular structure and a broader molecular weight distribution. On the other hand, hyperbranched polymers can be prepared through some relatively simple methods, such as one-step polymerization of AB_x-type monomers (where x is generally 2 or 3). The preparation does not need the tedious isolation and purification procedures required for preparing dendrimers through the generation-by-generation scheme.[10−14] Therefore, hyperbranched polymers are considered as a unique type of dendritic polymer, which possesses interesting properties of the dendritic structures and feasibility for large-scale manufactures at the same time.[15−20]

Polymers containing azobenzene-type chromophores (azo-polymers for short) have been extensively studied in recent years.[21−25] On the basis of the optically induced trans−cis isomerization of azo-chromophores, azo-polymers have been wildly investigated for diversified potential applications. The photoinduced isomerization can cause significant bulk and surface property variation of the polymers, such as photoinduced phase transition, photoinduced anisotropy, and photoinduced surface relief gratings (SRGs), among others.[26−31] For azo-polymers containing donor−acceptor-type azo-chromophores, the nonlinear optical property is another important function that has been well studied.[21] Polymers with such properties are promising for applications in holographic gratings, reversible optical storage systems, electrooptical (EO) modulators, and sensors. For decades, research efforts to explore new azo-polymers have predominantly focused on the linear azo-polymers with side-chain or main-chain architectures.[21−25] More recently, dendrimers containing azobenzene units have attracted considerable attention and have been intensively investigated. The dendrimers are designed to bear azo-chromophores in the exterior and interior or throughout the dendritic architecture.[32−34] Those azo-dendrimers have exhibited some fascinating properties, such as harvesting low-energy photons[35] and improving both the nonlinear optical properties and thermal stability of the azo-polymers.[34b,36] In contrast to the intensive study on the azo-dendrimers, only few hyperbranched azo-polymers have been synthesized and studied.[37,38]

Formation of photoinduced surface relief gratings (SRGs) is one of the most interesting properties of azo-polymers found in recent years.[24,30,31,39−41] By exposure of the polymer films to the interfering laser beams, SRGs are formed on the films at a temperature well below the glass transition temperatures (T_gs) of the samples. In contrast to irreversible surface patterns prepared by conventional methods such as chemical

* Corresponding author: Fax 86-10-62770304; e-mail wxg-dce@mail.tsinghua.edu.cn.

10.1021/ma0511393 CCC: $30.25
Published on Web 09/22/2005

etching and laser ablation, SRGs can be removed by heating samples to a temperature above their T_gs or erased optically even below the T_gs.[42,43] This function can be potentially applied to the fabrication of diffractive optical elements and waveguide couplers.[44−46] Since the phenomenon was reported, the factors controlling the SRG formation have been actively investigated. The SRG formation at low or middle light intensity is due to neither a thermally driven process nor the photoablation occurring in the irradiation regions.[24,47] The photoinduced dynamic process depends on the intensity and polarization state of the interfering beams, the thickness of the films, and the molecular weight of polymers.[40,43,47] The rate of the SRG formation and the modulation depth are also closely related to the polymer structure and the irradiating energy of the writing beam.[24,40,47,48] Although several models have been proposed to describe the SRG formation, no general agreement about the forming mechanism has been reached until the present time.[24,47] Hyperbranched azo-polymers are expected to show both SRG-forming ability and the interesting properties of dendritic polymers. Meanwhile, because of the significantly different molecular architecture compared to their linear analogues, study on the structure−property relationship of hyperbranched azo-polymers can shed new light on the molecular origin of the SRG formation. However, to our knowledge, no systematic study on the SRG properties of hyperbranched azo-polymers (or even other dendritic azo-polymers) has been reported, which is partly due to the lack of a straightforward way to prepare hyperbranched azo-polymers under mild conditions.

Recently, we found that hyperbranched azo-polymers can be obtained through azo-coupling reaction of an AB_2 monomer under extremely mild conditions.[49] For years, the azo-coupling reaction, which can be carried out in different ways, has been well developed to prepare various types of dyestuff.[22] By exploiting the knowledge base, a variety of hyperbranched azo-polymers can be designed and prepared. Through this scheme, the strict reaction conditions such as high temperature and vacuum can be avoided. Moreover, the hyperbranched azo-polymer contains a large amount of peripheral diazonium salt groups, which can be further modified to introduce other types of terminal groups.

In this work, we develop a new synthetic scheme through two-stage azo-coupling reactions based on a newly designed AB_2 monomer. A hyperbranched precursor azo-polymer (HPAP), which contains a large number of peripheral anilino groups, was prepared by step-growth polycondensation of the monomer through azo-coupling reaction. HPAP was further modified through postpolymerization azo-coupling reactions to introduce different peripheral azo-chromophores. The scheme can be used to prepare a variety of azo-polymers that have a highly branched azo-backbone and bear different types of azo-chromophores at the peripheral positions. In this paper, the synthesis and characterization of the monomer, the precursor polymer, and the hyperbranched azo-polymers are reported. Their SRG formation properties and their relationship with the molecular structure are discussed in detail.

Experimental Section

Characterization. ^{1}H NMR and ^{13}C NMR spectra were obtained on a JEOL JNM-ECA600 NMR spectrometer. The glass transition temperatures (T_gs) of the polymers were tested with a TA Instruments DSC 2910 at a heating rate of 10 °C/min under N_2 protection. The molecular weights and their distributions of the polymers were determined by gel permeation chromatography (GPC) utilizing a Waters model 515 pump and a model 2410 differential refractometer with three Styragel columns HT2, HT3, and HT4 connected in a serial fashion. THF was used as the eluent at a flow rate of 1.0 mL/min. Polystyrene standards with dispersity of 1.08−1.12 obtained from Waters were employed to calibrate the instrument. Infrared spectra were measured using a Nicolet 560-IR spectrometer by incorporating the sample in a KBr disk. Elemental analysis of C, H, and N was completed through the Heratus CHN-Rapid method. UV−vis spectra of the azo-polymers in solutions and as spin-coated films were recorded on a Perking-Elmer Lambda Bio-40 spectrometer. The surface images of the surface relief gratings were monitored using atomic force microscopy (AFM) (Nanoscope IIIa, tapping mode).

Materials. *N*-Ethyl-*N*-hydroxyethylaniline and 3,5-bis(carboxyl)aniline were purchased as commercial products from Acros. All other reagents and solvents such as dimethyl sulfoxide (DMSO) and *N*,*N*-dimethylformamide (DMF) were used as received without further purification.

***N*-Ethyl-*N*-(2-chloroethyl)aniline (ECA).** *N*-Ethyl-*N*-hydroxyethylaniline (18.2 g, 0.11 mol) was slowly added into a round-bottom flask containing phosphorus oxychloride (10.2 mL 0.11 mol) with ice bath cooling. After the addition was completed, the mixture was heated to 110 °C and reaction was carried out at this temperature for 1 h under a nitrogen atmosphere protection. Then the mixture was poured into benzene (50 mL). A proper amount of water (about 50 mL) was mixed with the benzene solution to extract the unreacted *N*-ethyl-*N*-hydroxyethylaniline and other water-soluble impurities. The aqueous layer was washed with benzene (5 mL) three times to extract the remaining product. The benzene solutions were mixed and dried with anhydrous magnesium sulfate. Oily product was obtained by removal of the benzene through vacuum evaporation. Yield 83%; bp 102−104 °C/399 Pa. IR (KBr): 2970 (s; C−H), 1600 1500 (s; benzene ring), 1340 (s; C−N) and 720 (s; C−Cl) cm^{-1}. ^{1}H NMR (DMSO-d_6): δ = 1.16 (t, −CH_3, 3H), 3.40 (m, N−CH_2CH$_3$, 2H), 3.60 (s, N−CH_2CH_2−Cl, 4H), 6.68 (m, Ar−*H*, 3H, ortho and para to N), 7.22 (t, Ar−*H*, 2H, meso to N). Elemental analysis: $C_{10}H_{14}$NCl (183.68) Calcd: C, 65.40; H, 7.87; N, 7.63; Cl, 19.30. Found: C, 64.10; H, 7.70; N, 7.81; Cl, 18.74.

Di[2-(*N*-ethylanilino)ethyl]-5-aminoisophthalate (DEEAP). DEEAP was prepared by the nucleophilic substitution reaction between ECA and 3,5-bis(carboxyl)aniline. ECA (1.835 g, 10 mmol) and 3,5-bis(carboxyl)aniline (0.724 g, 4 mmol) were dissolved in DMSO (50 mL) in a 250 mL round-bottom flask. Potassium carbonate (4 g) and potassium iodide (1 g) were added into the DMSO solution. The reaction was carried out at 110 °C for 7 h with stirring, and then the mixture was poured into an excessive amount of water. The precipitated DEEAP solid was collected by filtration and washed with plenty of water. The product was dried in a vacuum oven at 70 °C for 24 h. Yield 80%; mp 110−112 °C. IR (KBr): 3460 3373 (s; N−H), 2970 (s; C−H), 1700 (s; COOR), 1597 1506 (s; benzene ring), and 1348 (s; N−C). ^{1}H NMR (DMSO-d_6): δ = 1.11 (t, −CH_3, 6H), 3.40 (m, N−CH_2CH$_3$, 4H), 3.65 (t, −COOCH$_2$CH_2N−, 4H), 4.39 (t, −COOCH_2CH$_2$N−, 4H), 5.74 (s, Ar−NH_2, 2H), 6.58 (t, Ar−*H*, 2H, para to N), 6.74 (d, Ar−*H*, 4H, ortho to N), 7.15 (t, Ar−*H*, 4H, meso to N), 7.40 (s, Ar−*H*, 2H, ortho to NH$_2$ and ortho to COO−), 7.68 (s, Ar−*H*, 1H, para to NH$_2$ and ortho to COO−).

Hyperbranched Precursor Azo-Polymer (HPAP). DEEAP (1.900 g, 4 mmol) was dissolved in a homogeneous mixture of glacial acetic acid (20.0 mL) and sulfuric acid (1.4 mL). Aqueous solution of sodium nitride (0.345 g, 5 mmol) in 0.9 mL water was added dropwise into the DEEAP solution at 0 °C, and the solution was kept at this temperature for 5 min. Then the clear solution of the diazonium salt was added dropwise into DMF (60 mL) at 0 °C. The reaction was carried out with stirring at the temperature for 12 h. The solution was then poured into an excess amount of water. The precipitate was collected by filtration and washed with water repeat-

edly. After being dried, the product was dissolved in DMF (30 mL) again and then dropped into an excess amount of ethanol with stirring. The precipitate was collected by filtration, washed with ethanol, and then dried in a vacuum oven at 70 °C for 48 h. Yield: 78%. GPC: M_n 142 000, MWD 1.44. DSC: T_g 91 °C. ^{1}H NMR (DMSO-d_6): δ = 1.08, 3.38, 3.62, 4.43, 6.54, 6.73, 6.92, 7.11, 7.72, 8.33. ^{13}C NMR (DMSO-d_6): δ = 165.0, 153.2, 151.3, 148.0, 143.1, 131.6, 129.6, 126.7, 126.1, 116.2, 112.4, 112.1, 63.6, 48.6, 44.9, 12.5. UV−vis (DMF): 425 nm; UV−vis (film): 436 nm.

HPAP-NT. The diazonium salt of 4-nitroaniline was prepared by adding an aqueous solution of sodium nitrite (0.200 g, 2.9 mmol) dropwise into a solution of 4-nitroaniline (0.345 g, 2.5 mmol) in a homogeneous mixture of sulfuric acid (1 mL) and glacial acetic acid (10 mL). The mixture was stirred at 0 °C for 5 min. The diazonium salt solution was added dropwise into a solution of HPAP (0.972 g, 2 mmol) in DMF (50 mL) at 0 °C. After the reaction was carried out at 0 °C for 10 h, the mixture was poured into an excess amount of water. The precipitate was collected by filtration and washed with water repeatedly. After being dried, the product was dissolved in DMF (10 mL) again and then dropped into an excess amount of ethanol with stirring. The precipitate was collected by filtration, washed with ethanol, and then dried in a vacuum oven at 70 °C for 48 h. Yield: 76%. DSC: T_g 139 °C. ^{1}H NMR (DMSO-d_6): δ = 1.06, 3.45, 3.74, 4.45, 6.80, 7.73, 8.21. ^{13}C NMR (DMSO-d_6): δ = 165.0, 156.0, 153.2, 152.0, 146.7, 143.5, 131.4, 129.0, 126.4, 126.0, 125.0, 122.8, 112.2, 63.5, 48.2, 45.1, 12.5. UV−vis (DMF): 450 nm; UV−vis (film): 443 nm.

HPAP-CA. HPAP-CA was synthesized and purified via a procedure similar to that described above for the HPAP-NT preparation. In the reaction, the diazonium salt of 4-aminobenzenic acid (2.5 mmol) was reacted with HPAP (0.972 g, 2 mmol) to obtain HPAP-CA. Yield: 79%. DSC: T_g 167 °C. ^{1}H NMR (DMSO-d_6): δ = 1.08, 3.45, 3.76, 4.46, 6.86, 7.69, 7.99, 8.26. ^{13}C NMR (DMSO-d_6): δ = 166.6, 164.3, 154.9, 152.0, 151.2, 142.7, 130.7, 130.1, 129.0, 125.5, 125.2, 121.4, 111.4, 47.8, 44.4, 11.8. UV−vis (DMF): 432 nm; UV−vis (film): 424 nm.

HPAP-CN. HPAP-CN was synthesized and purified via a procedure similar to that described above for the HPAP-NT preparation. In the reaction, the diazonium salt of 4-aminobenzonitrile (2.5 mmol) was reacted with HPAP (0.972 g, 2 mmol) to obtain HPAP-CN. Yield: 80%. DSC: T_g 133 °C. ^{1}H NMR (DMSO-d_6): δ = 1.08, 3.47, 3.77, 4.42, 6.83, 7.77, 8.24. ^{13}C NMR (DMSO-d_6): δ = 165.0, 155.3, 153.2, 151.5, 143.3, 133.8, 131.4, 129.6, 126.7, 126.2, 122.8, 116.2, 112.5, 63.6, 48.7, 44.6, 12.5. UV−vis (DMF): 439 nm; UV−vis (film): 438 nm.

Preparation of Polymer Films. Suitable amounts of the polymer samples were dissolved in DMF to obtain solutions with concentrations about 0.1 g/mL. The solutions were filtered through 0.45 μm membranes. The films were prepared by spin-coating the solutions onto clear glass slides. By adjusting the spining rate, the thickness of the films was controlled to be about 1.0 μm. After dried at 70 °C under vacuum for 48 h, the films were stored in a desiccator for further studies.

Surface Relief Grating (SRG) Fabrication. The experimental setup for SRG fabrication was similar to those reported before.[30,31] A linearly polarized Ar^+ laser beam (488 nm, 150 mW/cm^2) was used as the light source. SRGs were optically inscribed on the polymer films with p-polarized interfering laser beams, where the Ar^+ laser beam was split by a mirror and the reflected half-beam coincided with the other half on the film surface. The surface profiles of the resulting gratings were recorded by using a Nanoscope atomic force microscope (AFM) in the tapping mode. The diffraction efficiency of the gratings was probed by measuring the first-order diffracted beam intensity of an unpolarized low power He−Ne laser beam (633 nm) in transmission mode. Even only weak absorption at the probed wavelength, the absorption effect of the polymer films was corrected in the calculation of the diffraction efficiency.

Scheme 1. Synthetic Route of the Precursor Hyperbranched Azo-Polymer

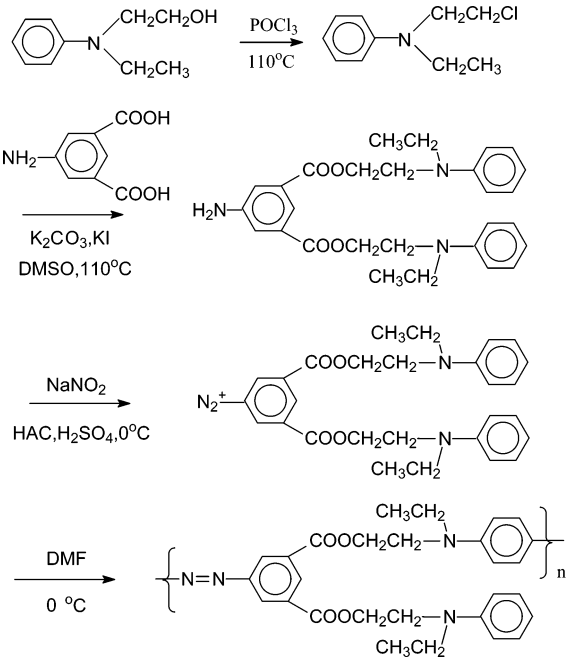

Scheme 2. Synthetic Route of HPAP-NT, HPAP-CA, and HPAP-CN

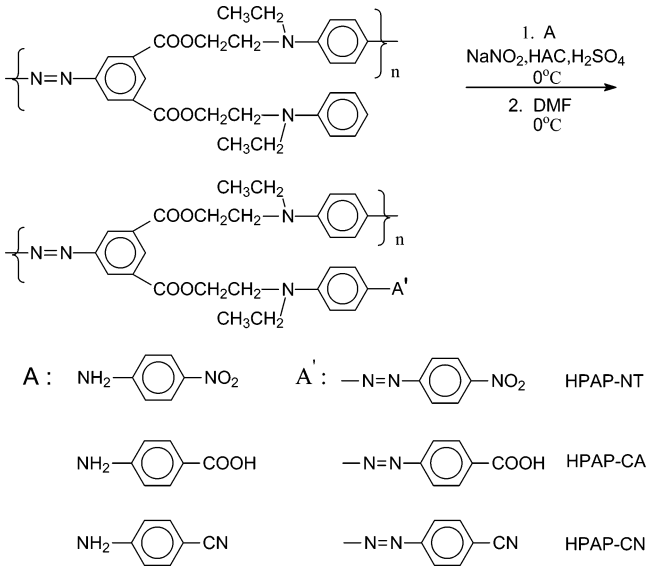

Results and Discussion

Preparation of Hyperbranched Azo-Polymers. The way to prepare the hyperbranched azo-polymers through the two-stage azo-coupling reactions is shown in Scheme 1 and Scheme 2. *N*-Ethyl-*N*-(2-chloroethyl)-aniline (ECA) was prepared by chloridizing *N*-ethyl-*N*-hydroxyethylaniline with phosphorus oxychloride ($POCl_3$). The AB_2 monomer, di[2-(*N*-ethylanilino)ethyl]-5-aminoisophthalate (DEEAP), was synthesized by nucleophilic substitution reaction between ECA and 3,5-bis(carboxyl)aniline in DMSO, using K_2CO_3 and KI as HCl absorbent and catalyst. The hyperbranched precursor azo-polymer (HPAP) was prepared by step-growth polymerization of DEEAP through azo-coupling reaction (Scheme 1). In the reaction, the diazonium salt of DEEAP was prepared and then added into a suitable amount of DMF with ice bath cooling. HPAP was obtained after reaction in DMF at 0 °C for 12 h. HPAP

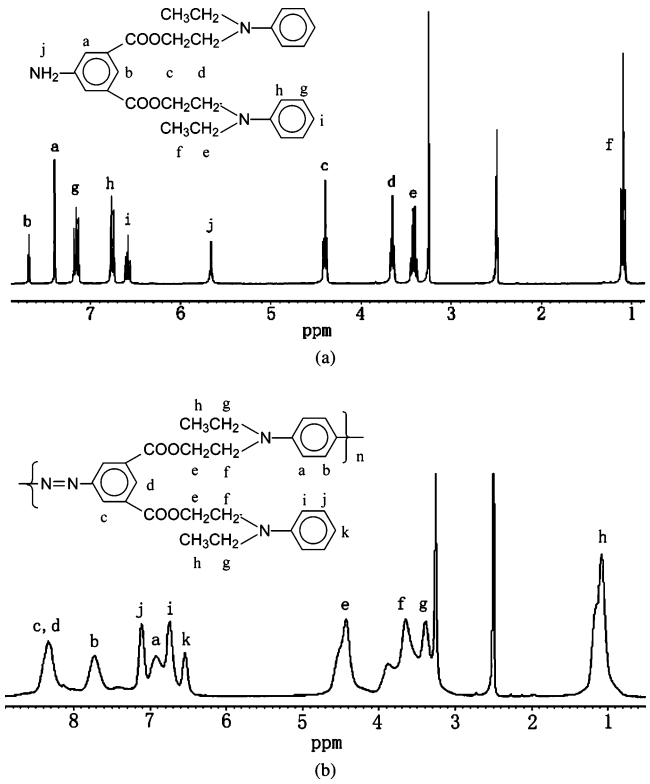

Figure 1. ^{1}H NMR spectra of (a) DEEAP and (b) HPAP in DMSO-d_6.

was further functionalized to incorporate three types of peripheral azo-chromophores by postpolymerization azo-coupling reactions (Scheme 2). In these reactions, HPAP was reacted respectively with the diazonium salts of 4-nitroaniline, 4-aminobenzoic acid, and 4-aminobenzonitrile in DMF to obtain HPAP-NT, HPAP-CA, and HPAP-CN.

^{1}H NMR spectra of the AB_2 monomer DEEAP and precursor polymer HPAP are given in Figure 1. In the spectrum of DEEAP (Figure 1a), the peak at 5.74 ppm corresponds to the resonance of the protons of the amino groups (protons Hj). After polymerization, the resonance disappears completely in the spectrum of HPAP (Figure 1b). Moreover, because of the increase of conjugated length and the introduction of strong electron-withdrawing groups, the chemical shifts of the protons of both *N*-ethylanilino and 5-aminoisophthalate moieties shift to lower magnetic field after forming the azo-linkages. In the ^{1}H NMR spectrum of HPAP, new peaks appearing at 8.33, 7.72, and 6.92 ppm are assigned to the resonances of the protons in azobenzene units. These spectroscopic characters clearly indicate that the amino groups of DEEAP reacted almost completely in the azo-coupling reaction, and an equal amount of azobenzene units was produced by the reaction. The number-average molecular weight (M_n) and the polydispersity index of HPAP, obtained by gel permeation chromatography (GPC), are 142 000 and 1.44. According to the GPC result, the average number of the monomer units in the polymer is estimated to be 290. The absorption band corresponding to the azobenzene units can be observed from the UV−vis spectrum of HPAP. Results obtained form^{1}H NMR, ^{13}C NMR, UV−vis, and GPC all suggest that the designed hyperbranched azo-polymer with a reasonably high molecular weight has been synthesized.

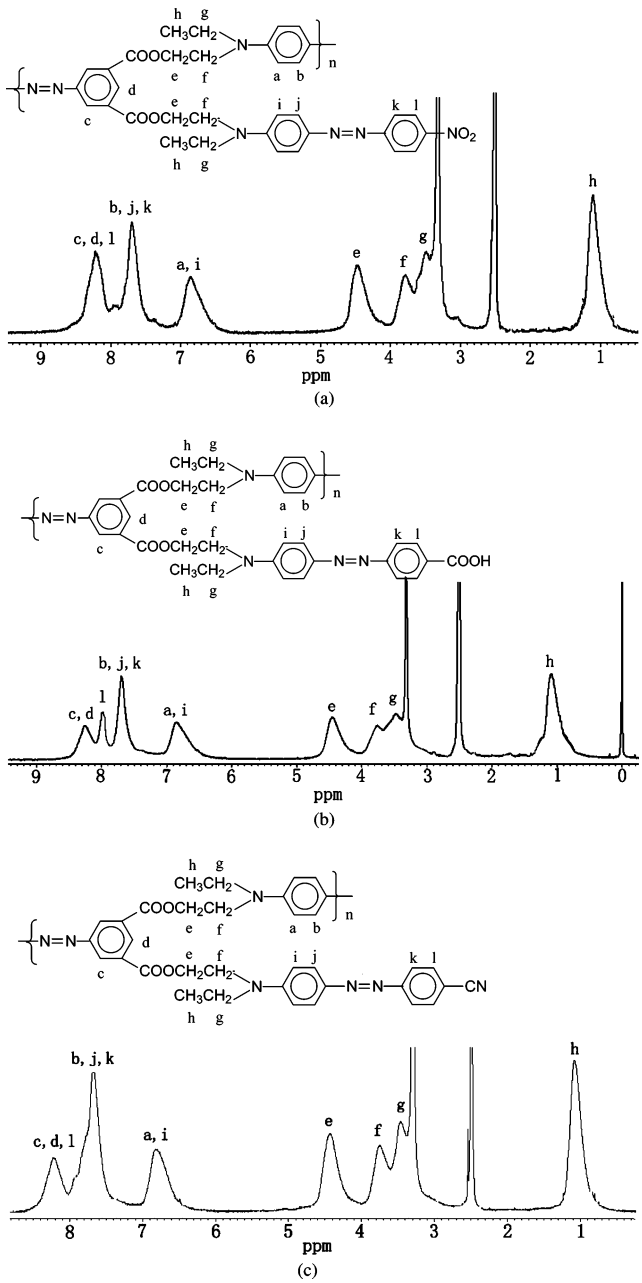

Figure 2. ^{1}H NMR spectra of (a) HPAP-NT, (b) HPAP-CA, and (c) HPAP-CN in DMSO-d_6.

^{1}H NMR spectra of HPAP-NT, HPAP-CA, and HPAP-CN are shown in Figure 2. The 6.54 ppm resonance (Figure 1b), corresponding to the protons in the para positions of the amino groups of the peripheral anilino moieties, disappears completely after the azo-coupling modifications (Figure 2a−c). Because of the presence of the electron-withdrawing groups introduced by the azo-coupling reactions, the resonances of the protons ortho and meta to the amino groups of the peripheral anilino moieties shift to lower magnetic field. These indicate that the peripheral anilino moieties are almost completely reacted, and the postpolymerization azo-coupling reactions occur at the para positions of peripheral aniline moieties of HPAP. According to those results, the reaction yields of the terminal anilino groups (the degree of functionalization) are about 100%. In our previous work, the postpolymerization azo-coupling reactions have been used to modify linear precursor polymers to incorporate azo-chromophores.[48,50] The cur-

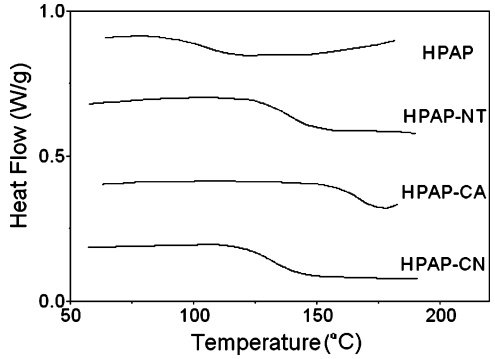

Figure 3. DSC curves of the hyperbranched azo-polymers.

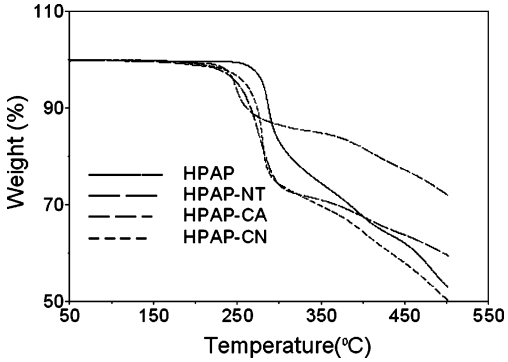

Figure 4. TGA curves of the hyperbranched azo-polymers.

Table 1. T_g and T_d of the Hyperbranched Azo-Polymers

polymer	T_g (°C)	T_d (°C)
HPAP	91	274
HPAP-NT	139	238
HPAP-CA	167	241
HPAP-CN	133	246

rent research shows that the same scheme can be successfully used to introduce various peripheral azo-chromophores into a hyperbranched precursor polymer.

Thermal Properties. The phase transition behaviors of the precursor polymer (HPAP) and the functionalized polymers (HPAP-NT, HPAP-CA, and HPAP-CN) were studied by using the differential scanning calorimetry (DSC). DSC curves of the hyperbranched polymers are given in Figure 3. All the hyperbranched polymers show the second-order phase transition of a typical amorphous substance. The glass transition temperatures (T_gs) of the polymers obtained by DSC are listed in Table 1. T_g of HPAP is about 91 °C. After introducing peripheral azo-chromophores, T_gs of the functionalized polymers become much higher than T_g of the precursor polymer. This is because of the significant increase both in the size and the dipole moment of the numerous terminal groups. The T_gs of HPAP-NT and HPAP-CN are 139 and 133 °C, which are about 48 and 42 °C higher than the precursor polymer. HPAP-CA exhibits the highest T_g of 167 °C among this series. The reason for such high T_g is attributed to intermolecular hydrogen bonding between carboxyl units of the terminal chromophores. The significant increase of T_g after postpolymerization azo-coupling reaction has been observed for linear epoxy-based polymers.[48,50] Introducing the azo-chromophores shows quite similar effect to increase the T_gs whether the azo-chromophores are in the side-chain positions or in the peripheral positions.

The thermal stability of the polymers was characterized by the thermogravimetric analysis (TGA). TGA curves of the precursor and functionalized polymers are shown in Figure 4, and the decomposition temperatures (T_ds) of the polymers are given in Table 1. The precursor polymer is thermally stable up to 274 °C under a nitrogen atmosphere. HPAP-NT, HPAP-CA, and HPAP-CN start to lose the weight at 238, 241, and 246 °C. After introducing the peripheral azo-chromophores, the thermal stability of the hyperbranched azo-polymers decreased.

Spectral Characteristics. Figure 5 shows the UV−vis spectra of the precursor polymer HPAP and the hyperbranched azo-polymers HPAP-NT, HPAP-CA, and HPAP-CN. Parts a and b of Figure 5 show spectra of the samples in the DMF solutions and as spin-coated thin films, respectively. The λ_{max} values of the polymers,

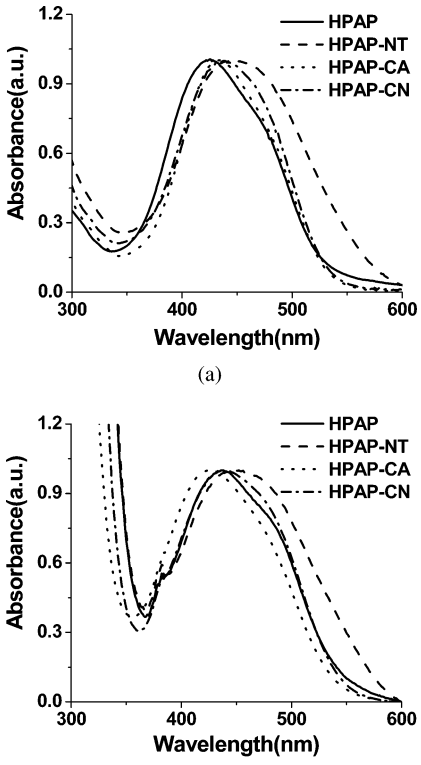

Figure 5. UV−vis spectra of the hyperbranched azo-polymers: (a) in DMF solutions and (b) as spin-coated films.

Table 2. λ_{max} of the Hyperbranched Azo-Polymers in DMF Solutions and as Spin-Coated Films

polymer	λ_{max} (nm) (in DMF solutions)	λ_{max} (nm) (as spin-coated films)
HPAP	425	436
HPAP-NT	450	443
HPAP-CA	432	424
HPAP-CN	439	438

corresponding to the $\pi-\pi^*$ transition, are listed in Table 2. As containing the donor−acceptor-type azo-chromophores, all the polymers show typical spectral characteristics of the pseudo-stilbene-type azo-chromophores.[21,23] For those azo-chromophores, the ($n-\pi^*$) state has a larger transition energy gap than that of ($\pi-\pi^*$) state. Therefore, the low-intensity $n-\pi^*$ band appears at a shorter wavelength than $\pi-\pi^*$ band and cannot be observed from the spectra. The spectrum of HPAP in the DMF solution shows the absorption maximum at 425 nm, and the λ_{max} red-shifts to 436 nm for the spin-coated film of the polymer. After incorporation of the peripheral azo-chromophores, UV−vis spec-

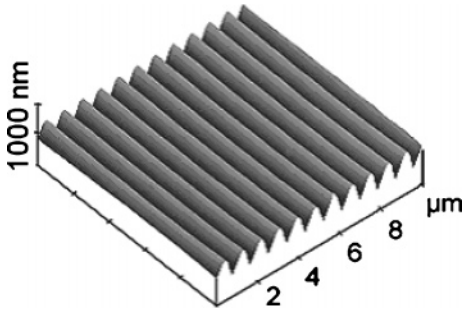

Figure 6. AFM image of the SRGs formed on HPAP-CA film (10.0 μm × 10.0 μm).

tra of HPAP-NT, HPAP-CA, and HPAP-CN show some significant differences. In addition to the azo-chromophores throughout the hyperbranched architecture, HPAP-NT, HPAP-CA, and HPAP-CN have another type of azo-chromophore at the terminal positions. The absorption bands of both types of azo-chromophores overlap, and only one broader peak can be observed in the spectra. The λ_{max} of the overlapped bands shifts to a longer wavelength or shorter wavelength, depending on the relative positions of the absorption bands of the internal azo-chromophores and the terminal azo-chromophores. The λ_{max} of HPAP-NT, HPAP-CA, and HPAP-CN in DMF solutions appears at 450, 432, and 439 nm. In contrast to HPAP, the λ_{max} of HPAP-NT, HPAP-CA, and HPAP-CN films shows a blue shift compared with the λ_{max} of the corresponding solution spectra, which appears at 443, 424, and 438 nm for HPAP-NT, HPAP-CA, and HPAP-CN solid films, respectively. The exact nature of this observation is not clear at the current stage. One possible explanation is that the absorption band shifts observed for the solutions and films are due to different mechanisms. When the environments of the polymeric chains change from solutions to solid films, the red shift of HPAP might be caused by a solvatochromic effect of the internal azo-chromophores, whereas the blue shift of HPAP-NT, HPAP-CA, and HPAP-CN could predominately result from the H-aggregation of the terminal azo-chromophores. The name H-aggregation originated in the observation of hypsochromic or H-bands in UV−vis spectra of ionic dyes, which mean those transitions that are blue-shifted and thus appear at shorter wavelengths than molecular absorption band (M-band).[51] The appearance of H-bands has been attributed to face-to-face aggregation through the formation of dimers, trimers, or even *n*-mers.[52,53] In the current case, the terminal azo-chromophores could form H-aggregates more easily in the solid states than in DMF solutions.

Surface Relief Grating (SRG) Behavior. Spin-coated thin films of the hyperbranched azo-polymers were used to carry out SGR inscription experiments. The experimental setup and conditions were similar to those reported before.[30,31] Two p-polarized Ar^+ laser beams (488 nm) were used to produce the interference pattern on the polymer films. Although using two circularly polarized interfering beams can produce SRGs more efficiently, the p/p-polarization condition has also been frequently used to fabricate good quality SRGs, and the result is relatively easier to be explained.[40,41] AFM observation indicated that sinusoidal surface relief structures with regular spaces were fabricated on the film surfaces of the azo-polymers. Figure 6 shows a typical AFM image of the surface structure formed on the HPAP-CA film after irradiated for 1000 s at room

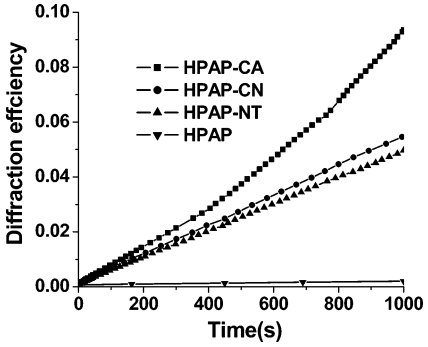

Figure 7. Diffraction efficiency of the surface relief gratings inscribed on the films of HPAP (▼), HPAP-NT (▲), HPAP-CN (●), and HPAP-CA (■) as a function of the irradiation time. The intensity of irradiation beam is about 150 mW/cm^2.

temperature. From the AFM measurement, the surface modulation depth is about 195 nm, and the grating spacing is about 890 nm. The modulation depth depends on the irradiation time, and the spatial period depends on both the angle θ between the two interfering beams and the wavelength λ of the writing beams. With the same irradiation time (1000 s), the modulation depth measured by AMF is significantly different for the films of HPAP, HPAP-NT, HPAP-CA, and HPAP-CN due to the different grating formation rates, which will be discussed in the following part.

The rates of grating formation can be probed by measuring the first-order diffraction efficiency of the SRGs during the grating inscription process.[30,31,40] In current study, the diffraction efficiency was recorded in-situ and used to characterize the rate of the surface modification. The rate of grating formation depends on both the structures of the polymers and the conditions such as film thickness, the light intensity, and the angle between the two interfering beams.[40] To attribute the difference of the SRG-forming rates only to the polymer structures, thick films (about 1 μm) were used and the other conditions were controlled to be the same in the experiments. Relatively low light intensity (150 mW/cm^2) was used to write the gratings in order to avoid the sample damage and the other possible side effects caused by high-intensity laser irradiation.

A plot of the diffraction efficiency as a function of the irradiation time for the hyperbranched azo-polymers is given in Figure 7. The precursor polymer HPAP exhibits the slowest inscription rate for the SRG formation among the four polymers. The rates of SGR formation are much faster for HPAP-NT, HPAP-CA, and HPAP-CN, which are functionalized by the peripheral azo-chromophores. It is obvious that the introduction of the terminal azobenzene chromophores increases the amount of azo-chromophores in the polymeric systems. It might be even more important that these peripheral azo-chromophores have less steric hindrance and are easier to undergo the photoinduced trans−cis isomerization. HPAP-CA, HPAP-NT, and HPAP-CN also show a considerable difference in the grating formation rates, in which the only structural difference distinguished with each other is the electron-withdrawing groups in the terminal azo-chromophores. With the same backbone structure, HPAP-CA shows the fastest inscription rate and HPAP-NT shows the slowest inscription rate among the series. HPAP-CN shows an intermediate inscription rate between those of HPAP-CA and HPAP-NT.

There is no directly comparable dendritic polymer system that has been reported before for the SRG study. One of the most closely related systems is a series of epoxy-based linear azo-polymers bearing the similar type azo-chromophores.[48] For the linear polymers, the rate of SRG formation is closely related with the electron-withdrawing groups in the azobenzene units. The linear polymers containing 4-carboxyazobenzene and 4-cyanoazobenzene groups show an obviously faster SRG formation rate than that of polymer containing 4-nitroazobenzene groups. In current study, a similar tendency was observed for the hyperbranched polymers containing those types of azo-chromophores in the terminal positions. Although hyperbranched azo-polymers are obviously different with their linear analogues in backbone architecture and located positions of the azo-chromophores, the influence of the electron-withdrawing groups appears to be the same.

Conclusions

A series of hyperbranched azo-polymers were prepared by step-growth polycondensation of an AB_2 monomer through the azo-coupling reaction and postpolymerization azo-coupling modification. This synthetic scheme can be used to prepare a variety of hyperbranched azo-polymers with different peripheral azo-chromophores under extremely mild conditions. Introducing the terminal azo-chromophores can significantly modify the thermal properties, spectral characteristics, and SRG formation behavior. The type of terminal azo-chromophores plays an important role to influence the rate of SRG formation. The hyperbranched azo-polymers can potentially be used for applications such as reversible optical data storage, photoswitching, sensors, and other photodriven devices.

Acknowledgment. The financial support from the NSFC under Project 50273018 and the MOST under Project 2002AA313130 is gratefully acknowledged.

References and Notes

(1) Kim, Y.; Webster, O. *Macromolecules* **1992**, *25*, 5561−5572.
(2) Inoue, K. *Prog. Polym. Sci.* **2000**, *25*, 453−571.
(3) Jikei, M.; Kakimoto, M. *Prog. Polym. Sci.* **2001**, *26*, 1233−1285.
(4) Gao, C.; Yan, D. *Prog. Polym. Sci.* **2004**, *29*, 183−275.
(5) (a) Mori, H.; Seng, D.; Zhang, M. *Langmuir* **2002**, *18*, 3682−3693. (b) Mori, H.; Seng, D.; Lechner, H.; Zhang, M. *Macromolecules* **2002**, *35*, 9270−9281.
(6) Kim, Y. *J. Polym. Sci., Part A: Polym. Chem.* **1998**, *36*, 1685−1734.
(7) Borkovec, M.; Koper, G. *Colloid Polym. Sci.* **1998**, *109*, 142−152.
(8) Hong, C.; Pan, C. *Polymer* **2001**, *42*, 9385−9391.
(9) Smits, R.; Koper, G.; Mandel, M. *Phys. Chem.* **1993**, *194*, 1953−1963.
(10) Yang, G.; Jikei, M.; Kakimoto, M. *Macromolecules* **1999**, *32*, 2215−2220.
(11) Miller, T.; Neenan, T.; Kwock, E.; Stein, S. *J. Am. Chem. Soc.* **1993**, *115*, 356−357.
(12) Kumar, A.; Ramakrishnan, S. *Macromolecules* **1996**, *29*, 2524−2530.
(13) Bolton, D.; Wooley, K. *Macromolecules* **1997**, *30*, 1890−1896.
(14) Turner, S.; Voit, B.; Mourey, T. *Macromolecules* **1993**, *26*, 4617−4623.
(15) Ding, J.; Chuy, C.; Holdcroft, S. *Chem. Mater.* **2001**, *13*, 2231−2233.
(16) Percec, V.; Kawasumi, M. *Macromolecules* **1992**, *25*, 3843−3850.
(17) Mathias, L.; Carothers, T. *J. Am. Chem. Soc.* **1991**, *113*, 4043−4044.
(18) Hawker, C.; Chu, F. *Macromolecules* **1996**, *29*, 4370−4380.
(19) Tuner, S.; Walter, F.; Voit, B.; Mourey, T. *Macromolecules* **1994**, *27*, 1611−1616.
(20) Hadjichristidis, N.; Pispas, S.; Pitsikalis, M.; Iatrou, H.; Vlahos, C. *Adv. Polym. Sci.* **1999**, *142*, 71−127.
(21) Xie, S.; Natansohn, A.; Rochon, P. *Chem. Mater.* **1993**, *5*, 403−411.
(22) Kumar, G. S. *Azo Functional Polymers: Functional Group Approach in Macromolecular Design;* Technomic Publishing Co. Inc.: Lancaster, 1993.
(23) Rau, H. *Photochemistry and Photophysics*; Rabek, J. F., Ed.; CRC Press: Boca Raton, FL, 1990; Vol. II, Chapter 4.
(24) Natansohn, A.; Rochon, P. *Chem. Rev.* **2002**, *102*, 4139−4175.
(25) Delaire, J. A.; Nakatani, K. *Chem. Rev.* **2000**, *100*, 1817−1845.
(26) Todorov, T.; Markovski, P.; Tomova, N.; Dragostinova, V.; Stoyanova, K. *Opt. Quantum Electron.* **1984**, *16*, 471−476.
(27) Ikeda, T.; Tsutsumi, O. *Science* **1995**, *268*, 1873−1875.
(28) Ichimura, K.; Oh, S. K.; Nakagawa, M. *Science* **2000**, *288*, 1624−1626.
(29) Hugel, T.; Holland, N. B.; Cattani, A.; Moroder, L.; Seitz, M.; Gaub, H. E. *Science* **2002**, *296*, 1103−1106.
(30) Rochon, P.; Batalla, E.; Natansohn, A. *Appl. Phys. Lett.* **1995**, *66*, 136−138.
(31) Kim, D. Y.; Tripathy, S. K.; Li, L.; Kumar, J. *Appl. Phys. Lett.* **1995**, *66*, 1166−1168.
(32) (a) Archut, A.; Vogtle, F.; Cola, L.; Azzellini, G.; Balzani, V.; Ramanujam, P.; Berg, R. *Chem.—Eur. J.* **1998**, *4*, 699−706. (b) Archut, A.; Azzellini, G.; Balzani, V.; Cola, L.; Vogtle, F. *J. Am. Chem. Soc.* **1998**, *120*, 12187−12191. (c) Schenning, A.; Elissen-Roman, C.; Weener, J.; Baars, M.; Gaast, S.; Meijer, E. *J. Am. Chem. Soc.* **1998**, *120*, 8199−8208. (d) Weener, J.; Meijer, E. *Adv. Mater.* **2000**, *12*, 741−746. (e) Nithyanandhan, J.; Jayaraman, N.; Davis, R.; Das, S. *Chem.—Eur. J.* **2004**, *10*, 689−698.
(33) (a) Junge, D.; McGrath, D. *Chem. Commun.* **1997**, 857−858. (b) Junge, D.; McGrath, D. *J. Am. Chem. Soc.* **1999**, *121*, 4912−4913. (c) Sidorenko, A.; Houphouet-Boigny, C.; Vilavicencio, O.; Hashemzadeh, M.; McGrath, D.; Tsukruk, V. *Langmuir* **2000**, *16*, 10569−10572. (d) Ghosh, S.; Banthia, A. *Tetrahedron Lett.* **2001**, *42*, 501−503.
(34) (a) Nagasaki, T.; Tamagaki, S.; Ogino, K. *Chem. Lett.* **1997**, 717−718. (b) Yokoyama, S.; Nakahama, T.; Otomo, A.; Mashiko, S. *Chem. Lett.* **1997**, 1137−1138. (c) Yokoyama, S.; Nakahama, T.; Otomo, A.; Mashiko, S. *J. Am. Chem. Soc.* **2000**, *122*, 3174−3181.
(35) Aida, T.; Jiang, D. *Nature (London)* **1997**, *388*, 454−456.
(36) Yokoyama, S.; Nakahama, T.; Otoma, A.; Mashiko, S. *Thin Solid Films* **1998**, *331*, 248−253.
(37) Wang, G. J.; Wang, X. G. *Chem. Lett.* **2002**, *1*, *78*−*79*.
(38) He, Y. N.; Wang, X. G.; Zhou, Q. X. *Synth. Met.* **2003**, *132*, 245−248.
(39) Ramanujam, P. S.; Holme, N. C. R.; Hvilsted, S. *Appl. Phys. Lett.* **1996**, *68*, 1329−1331.
(40) Tripathy, S. K.; Kim, D. Y.; Li, L.; Kumar, J. *CHEMTECH* **1998**, *28*, 34−40.
(41) Viswanathan, N. K.; Kim, D. Y.; Bian, S.; Williams, J.; Liu, W.; Li, L.; Samuelson, L.; Kumar, J.; Tripathy, S. K. *J. Mater. Chem.* **1999**, *9*, 1941−1955.
(42) Ho, M. S.; Barrett, C.; Paterson, J.; Esteghamatian, M.; Natansohn, A.; Rochon, P. *Macromolecules* **1996**, *29*, 4613−4618.
(43) Jiang, X. L.; Li, L.; Kumar, J.; Kim, D. Y.; Tripathy, S. K. *Appl. Phys. Lett.* **1998**, *72*, 2502−2504.
(44) Paterson, J.; Natansohn, A.; Rochon, P.; Callender, C.; Robitaile, L. *Appl. Phys. Lett.* **1996**, *69*, 3318−3320.
(45) Rochon, P.; Natansohn, A.; Callender, C.; Robitaile, L. *Appl. Phys. Lett.* **1997**, *71*, 1008−1010.
(46) Stockermans, R.; Rochon, P. *Appl. Opt.* **1999**, *38*, 3714−3719.
(47) Barrett, C. J.; Yager, K. G. *Curr. Opin. Solid State Mater. Sci.* **2001**, *5*, 487−494.
(48) He, Y. N.; Wang, X. G.; Zhou, Q. X. *Polymer* **2002**, *43*, 7325−7333.
(49) Che, P. C.; He, Y. N.; Zhang, Y.; Wang, X. G. *Chem. Lett.* **2004**, *33*, 22−23.
(50) Wang, X. G.; Kumar, J.; Tripathy, S. K.; Li, L.; Chen, J.; Marturunkakul, S. *Macromolecules* **1997**, *30*, 219−225.
(51) Herz, A. H. *Photogr. Sci. Eng.* **1974**, *18*, 323−335.
(52) McRae, E. G.; Kasha, M. *J. Chem. Phys.* **1958**, *28*, 721−722.
(53) DeVoe, H. *J. Chem. Phys.* **1964**, *41*, 393−400.

MA0511393